전압제어 유도 전동기를 위한 최적 PWM 스위칭 방법

한상수* · 추순남**

An Optimized PWM Switching Strategy for an Induction Motor Voltage Control

Sang-Soo Han* · Soon-Nam Chu**

요 약

유도 전동기를 전압 제어하기 위한 최적 PWM 스위칭 방법을 제시하려한다. 전압 인버터의 공간 벡터 변조 방식은 DC-버스 이용을 향상시키고 정류 손실을 감소시키기 때문에 디지털 구현의 경우 특히 선호하는 PWM 방법이다. 유도 전동기 전압 제어를 위한 최적 PWM 스위칭 방법은 제시한 최적 PWM 알고리즘을 사용하여 두 개의 활성 전압 벡터(active voltage vector)와 하나의 영 전압 벡터(zero voltage vector)로 구성하였다. 선택된 스위칭 순차 열은 변조 지수(modulation index)와 운송파(carrier wave) 주기의 함수로 정의 된다. 순차 열은 인버터 스위칭 손실과 전류 리플 값을 기준으로 사용하여 선택된다. 실험 결과 중·저 전력용으로 사용할 경우, 스위칭 주파수를 증가시킴에 따라 고조파 왜곡이 감소하고 동특성이 좋아짐을 확인할 수 있었다.

ABSTRACT

An optimized PWM switching strategy for an induction motor voltage control is developed and demonstrated. Space vector modulation in voltage source inverter offers improved DC-bus utilization and reduced commutation losses and has been therefor recognized the preferred PWM method especially in case of digital implementation. An optimized PWM switching strategy for an induction motor voltage control consists of switching between the two active and one zero voltage vector by using the proposed optimal PWM algorithm. The preferred switching sequence is defined as a function of the modulation index and period of a carrier wave. The sequence is selected by using the inverter switching losses and the current ripple as the criteria. For low and medium power application, the experimental results indicate that good dynamic response and reduced harmonic distortion can be achieved by increasing switching frequency.

키워드

Space vector modulation, Optimized PWM switching strategy, Inverter switching losses, Current ripple

* 경원대학교 IT대학 정보통신공학과
** 경원대학교 공과대학 전기공학과

접수일자 2008. 11. 26
심사완료일자 2009. 01. 12

Ⅰ. Introduction

The purpose of PWM is to generate an output waveform with desired frequency and magnitudes with a composition pulses of variable width form a given constant magnitude input. Even thought the output voltage waveform of idea inverters should be sinusoidal, the waveform of practical inverters is non-sinusoidal and contain harmonics [1].

During the last decade, various PWM switching strategies have been proposed and developed. Modern AC drives with gate-commutated switches use various PWM methods for voltage or current control.

The desirability of a given method depends on :

- harmonic distortion of the output waveform for a given switching frequency
- utilization of a DC bus voltage
- dynamic response
- ease of implementation

The most preferred PWM technique today is space vector modulation[2], [3], [4] which offers 15% better bus utilization and 33% fewer commutations per cycle than conventional PWM. Since the space vector modulation offers superior performance with respect to other modulation technique, both establishing the sequencing strategy in microprocessor- implemented PWM control scheme which is the best suitable for variable frequency AC drives and developing an efficient and simple strategy to obtain the desired performance criteria are equally important.

Analytical expression is derived for the RMS value of the current ripple as a function of the modulation index. Experimental data consist of the stator current waveform of an induction motor, its line voltage spectra.

In the proposed scheme, the switching patterns are directly generated by means of on-line computations and stored by look-up table memory. The system memory requirement and CPU time are reduced because the scheme only needs the precalculation of a minimum number of switching points per half cycle. The switching strategies are determined by varying the modulation index, M, and period of a carrier wave, T.

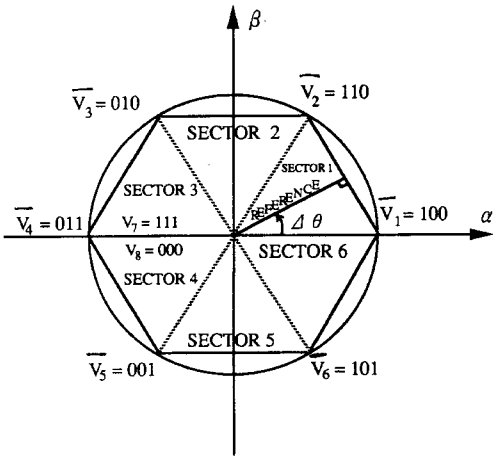

그림1. α-β 고정 프레임에서의 인버터 벡터 $\overline{V_1}$,… $\overline{V_8}$의 위치

Fig.1 Location of the inverter vectors $\overline{V_1}$,… $\overline{V_8}$ in the α-β stationary frame

Ⅱ. Space vector modulation

A three-phase invertor can assume 8 different switching states, corresponding to 7 discrete voltage vectors at output as shown in Fig.1.

The PWM strategy defines the sequencing of the available vectors in such a way that the average voltage within one cycle corresponds to the reference $\overline{U}$. The cycle time T is defined as the time necessary to go through the sequence of three successive vectors(interval T in Fig.2). The cycle T can also be defined as the minimum interval where the average inverter output corresponds the reference $\overline{U}$.

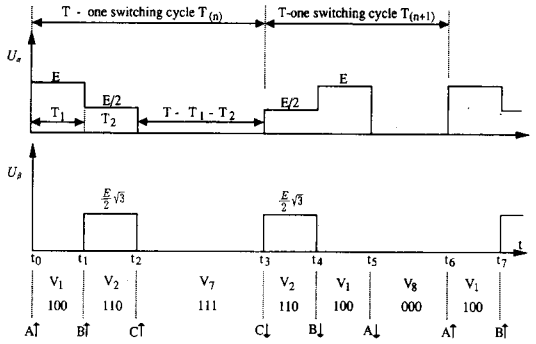

그림2. 섹터1에서 기준벡터와 제시한 스위칭 열을 갖는 공간벡터 변조 시간도

Fig.2 Timing diagram for space vector modulation with proposed switching sequence and a reference vector in sector 1

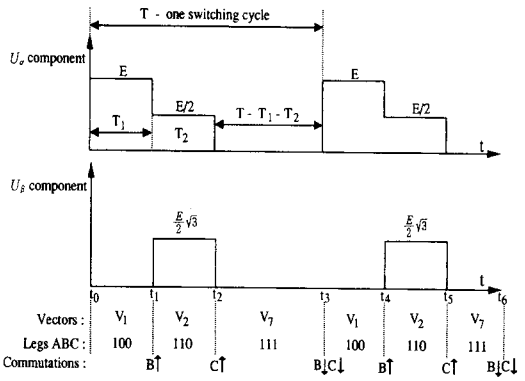

그림3. 섹터1에서 기준벡터와 일반 스위칭 열을 갖는 공간 벡터 변조의 시간도

Fig3. Timing diagram for space vector modulation with regular switching sequence and a reference vector in sector 1

The space vector modulation and problem of selecting the appropriate switching sequence are clearly understood if the phase quantities are transformed into the α-β stationary reference frame :

$$U_\alpha = -\frac{U_a + U_c}{2}, U_\beta = \frac{\sqrt{3}}{2} \times (U_b - U_c) \qquad (1)$$

Table 1 gives the α and β components of each voltage vector, together with switching states for all six segments defined in Fig.1. E denotes the DC-bus voltage.

표1. 인버터 출력에서 전압벡터의 정의, α , β성분 그리고 인버터 스위칭 상태

Table 1. Definition of the voltage vectors available at inverter output, their α and β components and the inverter switching states

VECTOR	ANGLE	U_α	U_β	STATES (*) 1 = HIGH ON 0 = LOW ON A	B	C	$\lvert \vec{U}_{\alpha\beta} \rvert$
$\vec{V}_1$	0°	E	0	1	0	0	E
$\vec{V}_2$	60°	$\frac{E}{2}$	$\frac{E}{2}\sqrt{3}$	1	1	0	E
$\vec{V}_3$	120°	$-\frac{E}{2}$	$\frac{E}{2}\sqrt{3}$	0	1	0	E
$\vec{V}_4$	180°	- E	0	0	1	1	E
$\vec{V}_5$	240°	$-\frac{E}{2}$	$\frac{-E}{2}\sqrt{3}$	0	0	1	E
$\vec{V}_6$	300°	$\frac{E}{2}$	$\frac{-E}{2}\sqrt{3}$	1	0	1	E
$\vec{V}_7$	-	0	0	1	1	1	0
$\vec{V}_8$	-	0	0	0	0	0	0

The non-zero vectors $\overline{V_1}, \cdots, \overline{V_6}$ create a hexagon as shown in Fig.1. The zero voltage vectors are located in the origin of the α-β plain. The modulation can be arranged in such a way that the output voltage $\overline{U_{\alpha\beta}}$ tracks the hexagon boundaries, but the voltage components $\overline{U_\alpha}$ and $\overline{U_\beta}$ will be non-sinusoidal.

The best tracking of the reference voltage $\overline{U}$ is obtained when the switching sequence includes only two vectors adjacent to $\overline{U}$ and a zero vector[3], [4].

As shown in Fig.2, the time intervals T_1, T_2 and T_0 determine the duration of the three vectors that compose the switching sequence.

These intervals depend on the amplitude and the spatial orientation of the reference vector $\overline{U}$.

Assuming that the reference $\overline{U}$ is in sector 1, at Fig.1, the time intervals T_1, T_2 and T_0 are given :

$$T_1 = T \cdot m \cdot \sin(60° - \Delta\theta) \quad (2)$$

$$T_2 = T \cdot m \cdot \sin(\Delta\theta) \quad (3)$$

$$T_0 = T - T_1 - T_2 \quad (4)$$

where, A : voltage vector amplitude,

$m = A/d$: modulation index,

$d = E \cdot \sin(60°)$: The radius of an inscribed circle in the hexagon,

$\Delta\theta = \arg(\overline{U}) - \arg(\overline{V_1})$: The displacement between the reference $\overline{U}$ and the clockwise side $\overline{V_1}$ vector.

The same rule (2)-(4) defines the intervals T_n, T_{n+1} and T_0 for any other sector in the hexagon. Depending on the spatial orientation of the voltage reference $\overline{U}$, each modulation cycle should consist of the sequence of vectors $\overline{V_n}, \overline{V_{n+1}}$ and $\overline{V_{7/8}}$, where $n \in [1,2,\cdots,6]$ is the sector number, while the angle $\Delta\theta = \arg(\overline{U}) - (n-1) \times 60°$. The zero vector is applied to the inverter output during the interval $T_0 = T - T_1 - T_2$ in each cycle.

As shown in Fig.2, in the transferring from one to the other state, the switching sequence between the three voltage vectors involves only one commutation.

This obviously requires the use of both zero vectors ($\overline{V_7}$ and $\overline{V_8}$) in a given sector and a reversal of the switching sequence every cycle. The benefit is the reduction of commutation from four th three comparing to a regular sequence in Fig.2 and 3.

The space vector modulation with cycle frequency $f_c = \frac{1}{T}$ has the same number of inverter switching as the SPWM(Sinusoidal Pulse Width Modulation) with the carrier frequency, $f_{PWM} = \frac{f_c}{2}$.

Ⅲ. The RMS values of the current ripple

From Fig.2, it is clear that the ripple waveform will be a periodic function with a period 2T. Neglecting the stator resistance and assuming the switching cycle T is essentially small with respect to the motor dynamics, the motor current will change linearly. Hance, the current values from t_3 and t_6 are calculated th be :

$$i_\alpha(t_4) = I_{\alpha 0} + (\frac{E}{2} - \frac{2m}{4})\frac{mTE}{2L\sigma} \quad (5)$$

$$i_\beta(t_4) = I_{\beta 0} + (\frac{\sqrt{3}}{2})\frac{mTE}{2L\sigma}(1 - \frac{m}{2}) \quad (6)$$

$$i_{\alpha\beta}(t_5) = i_{\alpha\beta}(t_2) \quad (7)$$

$$i_{\alpha\beta}(t_0) = i_{\alpha\beta}(t_3) = i_{\alpha\beta}(t_6) = [I_{\alpha 0}, I_{\beta 0}] \quad (8)$$

where, $i_\alpha(t_0) = I_{\alpha 0}$, $i_\beta(t_0) = I_{\beta 0}$: initial values,

L_σ : The motor equivalent leakage inductance,

m : modulation index,

E : DC-bus voltage,

T : cycle period.

The average value of α and β current components in the interval $[t_0, \cdots t_6]$ of the proposed sequence(Fig.3) are given by :

$$i_\alpha^{av}(t_0, t_6) = \frac{mTE}{2L\sigma} \cdot \frac{3}{4}(1-m) + I_{\alpha 0}$$

$$i_\beta^{av}(t_0, t_6) = \frac{\sqrt{3}}{4}\frac{mTE}{2L\sigma}(1-m) \quad (9)$$

The RMS values of the α and β ripple components are given by :

$$\Delta i_{\alpha s}^2 = \frac{1}{2T}\int_{t_0}^{t_6} i_\alpha^2(t)dt - (i_\alpha^{av})^2 \quad (10)$$

$$\Delta i_{\beta s}^2 = \frac{1}{2T}\int_{t_0}^{t_6} i_\beta^2(t)dt - (i_\beta^{av})^2 \qquad (11)$$

The total ripple RMS value is given by :

$$\Delta i_{\alpha\beta s}^2 = [\frac{mTE}{2L\sigma}]^2[\frac{1}{4} - \frac{5m}{12} + \frac{m^2}{4}] \qquad (12)$$

Ⅳ. Optimized PWM switching strategy for microprocessor based implementation

An Z-80A microprocessor-based inverter controller is built to optimized PWM switching sequence. The block diagram of the implementation system is shown in Fig.4.

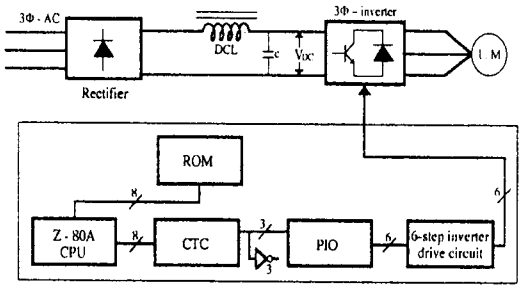

그림4. Z-80A 마이크로프로세서 기준 3φ-PWM인버터의 블럭도
Fig.4. The block diagram of an Z-80A microprocessor-based 3φ-PWM Inverter

The determinations of intervals T_n, T_{n+1} and T_0 are difficult for the microprocessor-based implementation, since the microprocessor requires powerful arithmetic capabilities and large memory space to store pulse width for a wide range of output voltage and frequency.

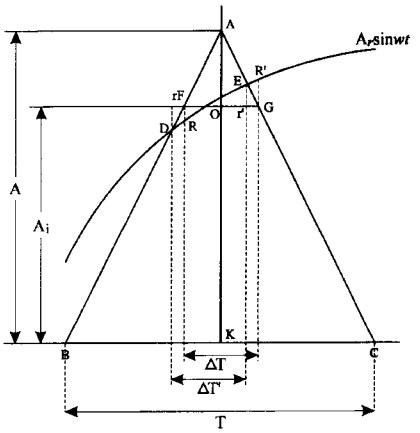

그림5. 제시한 PWM파 발생 방법
Fig.5. Proposed PWM wave generation strategy

To save the CPU time and look-up table memory and to avoid floating point operation, the minimum number of pulse per half-cycle, P, which to calculate the pulsewidths in the proposed technique, is determined by :

$$P = \frac{f_c}{2f_r} = 9 + 6(K-1) \qquad (13)$$

where, $K = 1, 2 \cdots, n$: integer,
f_c : The frequency of a triangular wave,
f_r : The frequency of a sine wave.

The modulation index, M is defined as :

$$M = \frac{A_r}{A_c} \qquad (14)$$

where A_c = The peak of carrier wave,
A_r = The peak of sine wave.

As shown in Fig.5, under $f_c > f_r$ condition, the reference wave between the two intersection points D and

E can be picewise linear. Therefore, the pulsewidths given by the space vector modulation method, $\sigma T'$, and the proposed method, ΔT, are approximately equal.

$$\Delta T' \equiv \Delta T \tag{15}$$

From the similarity between ΔAFO and ΔABK in Fig.5, the following relation can be achieved :

$$\frac{1}{2}\Delta T : \frac{1}{2}T = (A_c - A_i) : A_c \tag{16}$$

where, A_i = The magnitude of i-th sine wave at the center point of i-th triangular wave, $i = 1,2,3\cdot\cdot\cdot,[P/2+1]$, $[\cdot]$ = Gauss operator.

From (16), i-th pulsewidth, ΔT_i, is given by :

$$\Delta T_i = T(1 - \frac{A_r}{A_C}) \tag{17}$$

From (14) and (16), the simple analytic from of equation (17) is obtained :

$$\Delta T_i = T(1 - \frac{A_r}{A_c}M) \tag{18}$$

As shown in Fig.6, the time intervals, ΔT_{ti}, between the i-th and (i+1)-th pulsewidth is given by :

$$\Delta T_{ti} = T(1 + \frac{A_i + A_{i+1}}{2A_r}M) \tag{19}$$

where, $t_i = 1,2,\cdot\cdot\cdot i-1$.

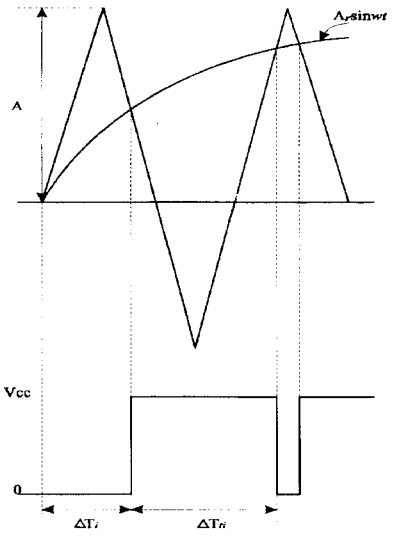

그림6. 기준 싸인파의 반주기동안의 게이트 신호 ΔT_i 와 ΔT_{ti}

Fig.6. The gate signals ΔT_i and ΔT_{ti} during the positive-half cycle of reference sine wave

During the positive-half cycle of reference sine wave, the driving transistor gate signals are generated by following operation :

TR On during the time interval of ΔT_i

TR Off during the time interval of ΔT_{ti}

During the magnitude-half cycle of reference sine wave, opposite gate signals are generated.

V. Analytical and experimental results

Analytical results for the RMS value of the motor current ripple are shown in Fig.7. If both regular and optimized strategies have the same switching cycle, T, as shown in Fig.2 and 3, the optimized strategies approach will have 25% fewer commutation but will have an increasingly larger ripple than the regular strategy for m>0.28, as the ripple for reducing the number of commutation. Trace C in Fig.7

corresponds to the optimized sequence with a reduce cycle time, $T' = 0.75T$, having the same commutation frequency as the regular sequence, trace A, but will have an increasingly larger ripple than the regular strategy for m>0.75. Trace D in Fig.7 with a reduce cycle time, $T' = 0.5T$ has 25% fewer commutation frequency than trace A but will have lower ripple than the regular sequence over the full voltage range.

The traces in Fig.7 suggest that the best result is obtained by the optimized strategy with a reduced cycle time, $T' = 0.5T$.

By reducing the cycle time T, the motor current ripple is reduce as shown in Figs.8-10, but switching losses are increased with the number of commutation.

Experimental result of the motor phase current and the line voltage spectra are shown in Fig.8-13. The phase current waveform for m=0.8 is shown in Figs.8-10. At the rated speed, it can be seen that the optimized sequence results in a significantly lower current ripple by reducing the cycle time, T.

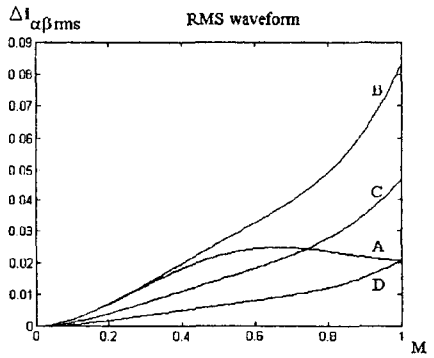

그림7. 변조지수 m의 함수로서 전류리플의 RMS값 A추이 : 정규 스위칭인 경우, B추이 : 최적화 스위치인 경우, C추이 : 주기시간 $T' = 0.75T$로 감소한 경우 최적화 스위치인 경우, D : 주기시간 $T' = 0.5T$인 경우

Fig7. The RMS value of the current ripple as a function of the modulation index, m. Trace A : with regular sequence, trace B : with optimized sequence, trace C : optimized sequence with reduced cycle time, $T' = 0.75T$; trace D : with cycle time, $T' = 0.5T$.

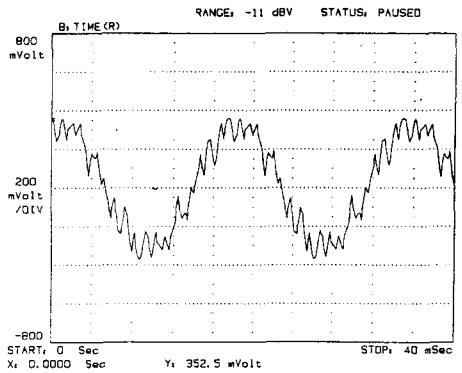

그림8. m=0.8, p=9인 경우 모터 상 전류

Fig.8. Motor phase current, m=0.8, p=9, proposed sequence

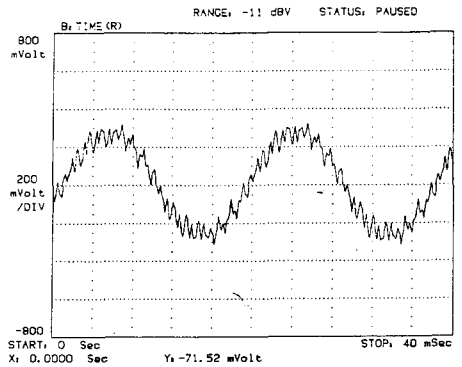

그림9. m=0.8, p=15인 경우 모터 상 전류

Fig.9. Motor phase current, m=0.8, p=15, proposed sequence

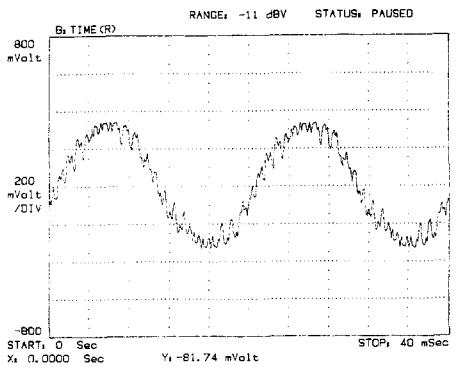

그림10. m=0.8, p=21인 경우 모터상 전류

Fig.10. Motor phase current, m=0.8, p=21, proposed sequence

The line voltage spectra of the waveforms in Figs.8-10 are obtained numerically and are given in Figs.11-13.

In Fig.11, the line voltage spectrum has a predominant components at the synchronous frequency of 57Hz, and a relatively small component at 63Hz. This small component is due to the relatively large harmonic distortion and current ripple.

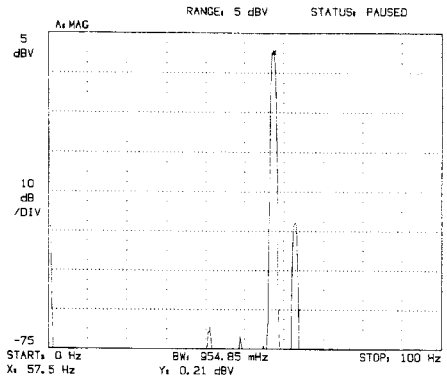

그림11. 그림8에서 보여준 선전압의 스펙트럼
Fig.11. Spectrum of the line voltage shown in Fig.8

In Figs.12-13, predominant components are located at about 50Hz, and relatively small components at about 70Hz.

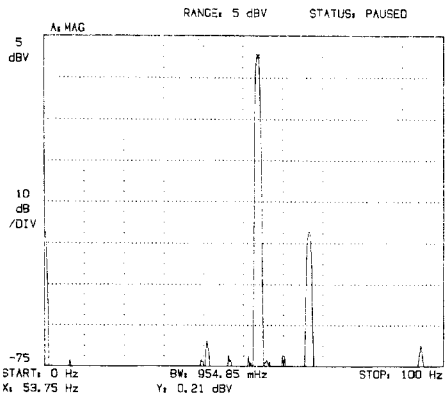

그림12. 그림9에서 보여준 선전압의 스펙트럼
Fig.12. Spectrum of the line voltage shown in Fig.9

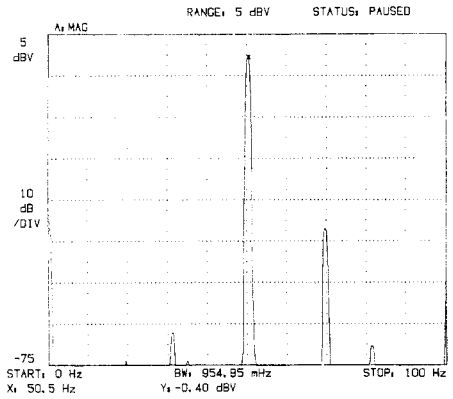

그림13. 그림10에서 보여준 선전압의 스펙트럼
Fig.13. Spectrum of the line voltage shown in Fig.10

Thus, these large bandwidths between the main components and relatively small components are due to small harmonic distortion and current ripple. However, by reducing the cycle time, T, the synchronous frequency is lower than the rated frequency of 60Hz because of increasing the slip. Therefor, for maintaining V/f=constant, the motor current should be controlled by adjusting the DC generator.

VI. Conclusion

Characteristics of regular and proposed PWM sequence strategies are investigated both analytically and experimentally. Experimental results are obtained by varying the cycle time with respect to the current ripple, the line voltage spectrum, and the commutation losses.

The developed technique is particularly suitable for a minimal size memory microprocessor implementation. Since the proposed switching sequence is defined by simple analytic expressions, and required the minimum number of pulse per half-cycle for the calculation of the pulsewidth.

For the modulation index, m, is less than 0.8, the proposed modulation strategy offers superior performance for majority of loads such as induction motor drives.

Reference

[1] T.L.GRANT and T.H.BARTON, "Control strategies for PWM drivers", IEEE Trans., Vol. IA-16, pp. 211-215, 1980.

[2] A,J.Pollman, "Software Pulsewidth Modu- lation for microprocessor Control of AC Drivers", IEEE Trans. Ind. Appl., Vol. IA-22, No. 4, pp. 691-696, July/Aug. 1986.

[3] J.Holtz, P.Lammert and W.Lotzkat, "High Speed Drive System with Ultrasonic MOSFET PWM Inverter and Single- Chip microprocessor Control", IEEE Trans. Ind. Appl., Vol. IA-23, No. 6, pp. 1010-1015, Nov/Dec. 1987.

[4] H.W.Van der Broeck, H.C.Skudelny and G.V.Stanke : "Analyses and Realization of a Pulsewidth Modulator Based on Voltage space Vectors", IEEE Trans. Ind. Appl., Vol. IA-24, No.1, pp. 142-150, Jan/ Feb. 1988

저자소개

한상수(Sang-Soo Han)

1982년 명지대학교 전자공학과 학사
1985년 명지대학교 전자공학과 공학석사
1995년 홍익대학교 전자공학과 공학박사

현재 : 경원대학교 IT대학 정보통신공학과 정교수
※관심분야 : 지능 및 퍼지제어, 전력전자제어, 로봇제어

추순남(Soon-Nam Chu)

1980년 명지대학교 전자공학과 학사
1983년 명지대학교 전자공학과 공학석사
2002년 경원대학교 전기공학과 공학박사

현재 : 경원대학교 공과대학 전기공학과 정교수
※관심분야 : 전력시스템, 전력전자재료